MIT
Center for Space Research

Chandra X-Ray Center

MEMORANDUM
February 16, 2000

To:	M.Elvis/SDSP Group Leader
From:	D.Davis/SDSP
Subject:	CXC Grating LSF Library & Tools Technical Reference
Cc:	C.Canizares/MIT-CXC Director F.Seward/User Support Group Leader

Transmission Grating Line Spread Function: Library and Tools Technical Reference

The purpose of this document is to provide a technical reference for the LSF/RMF reference data and software for analysis of the transmission grating data from the Chandra X-ray Observatory (CXO) and a summary of the LSF/RMF tools for the gratings and the RMF derived from the LSF reference data as they currently exist. The target audience is assumed to have experience with X-ray data analysis methods, the scientific ramifications of the analysis methods, and software.

1 Introduction

Here we give an overview of the method we use to generate the LSF used in analysis, how to apply the LSF and the derived products (eg. RMF) to analysis and a synospsis of the caveats that may effect the fitting of the data. Figure 1 shows the flow of data needed to prepare reference data for use in the analysis of CXO grating data. The starting point for this analysis are calibration derived MARX parameters and input data. These are changed when calibration updates are released. These CIP (Calibration Interface Products) are then used to generate MARX simulations which are used to characterize the HRMA + HETG or HRMA + LETG Line Spread function. These MARX simulations need further processing to convert them into products that the DS can use for analysis and for the convenience of the user. The products derived for the user are 1) the LSF library files, 2) the RMF files, and 3) the encircled energy (EE) library files.

The LSF library files are a one dimensional projection of the MARX events. This projection is done either in the dispersion direction (along the spectrum) or in the cross-dispersion direction (across the spectrum) and the events are binned into 1 μm pixels. These profiles are then repackaged into the DS LSF library format and are available in The Grating's PSF Library,

`http://hea-www.harvard.edu/asclocal/sds/ICD/index.html`

These library files are currently used by PSF_Model which will return an LSF for a specific energy and zero order position and by PSF_Frac which will integrate the profile to determine the encircled energy fraction for a given radius.

The RMF files are the most familiar files for most X-ray spectral work. These are derived from the MARX 2D LSF data by fitting Gaussians LSF. The fits are then used in RSPgen (GSFC tool) to create RMF's for fitting extracted spectra. These RMF can be currently used with Sherpa or with XSPEC to fit lines in the extracted spectra, to fit models to the spectra or portions of the spectra.

The EE tables created from 1-D products mainly exist for use with the user tool, PSF_Size, to estimate the extent of a feature in the grating data. These tables will be used in future versions of the grating analysis tools (eg. to create shaped extraction regions).

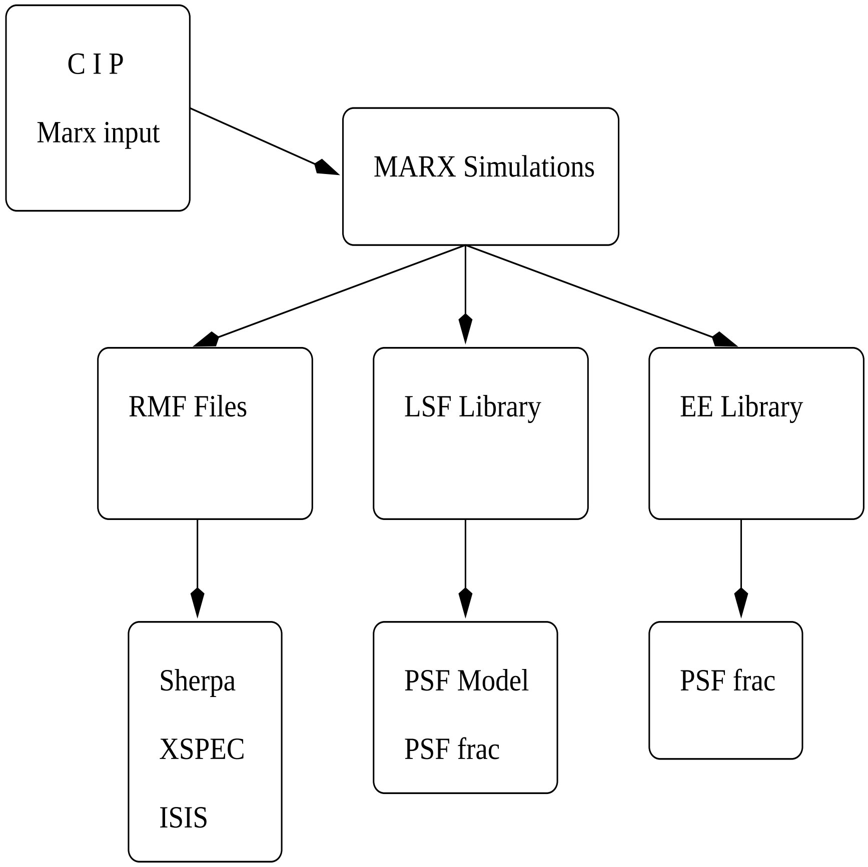

Figure 1: Diagram showing the flow of reference data from the Calibration Input file to the final products and a few of the tools which use this data to analyze CXO grating products.

2 Generation of Reference Data

2.1 Simulations

The LSF's were generated using MARX v2.2 and the internal MARX mirror model as well as the model for the HETG or LETG to describe the redistribution of photons from a point source. The input parameters for the simulations used the nominal set of input parameters so that the output does not reflect any calibration uncertainties. While the MARX mirror model does not reproduce all the features contained in the more detailed SAOsac raytrace model, it does include all the important effects and for the integrated properties is an excellent description (see the MARX manual and `Calibration Document TBD` for more details).

2.2 Line Spread Function

We use the term Line Spread Function (LSF) to describe the redistribution of photons from a source which is a delta function, spectrally and spatially, and integrated in either the dispersion or cross-dispersion direction. The product caclulated here is from the HRMA and the gratings but does not currently include aspect or processing effects. The integration region is $\pm$ 5.3$''$ for the dispersion and cross-dispersion data which includes most of the power in the line. A few tenths of a percent of the total number of photons are scattered outside this integration region.

In flight the spectra of celestial sources has contributions from several sources which affect the LSF. The most important is the blurring introduced by the mirror (the HRMA PSF) and is discussed in `Calibration Document TBD`. The HRMA PSF is further blurred by the redistribution from the transmission gratings. Additional blurring is introduced from errors in the aspect solution and pixelization of the detector.

2.3 Generation of the LSF Library and RMFs

The LSF library is generated from MARX simulations that are run for several locations: 0, 1, 2, 4, 6, 8, 16$'$ in azimuth and 0, 1, 2, 4, 6$'$ in altitude and contain $\sim 10^5$ counts. The MARX data files are read into IDL and a square region 5$''$.3 on a side, centered on the position of the line and with 1 μm pixels is extracted. This region is then integrated in the dispersion or cross-dispersion direction to obtain the LSF or the cross-dispersion profile. These profiles are then reformatted into the FITS library format described in PSF Library ICD `http://icxc.harvard.edu/icd/HTML/index.html`.

The current version of the RMF generation program for the grating RMF's produces RMF from a series of Gaussian functions. To accommodate this the HETG LSF data were fit with a Gaussian function (see §3). These fitted functions were then used to construct the HEG and MEG RMF's. The Gaussian functions for the LETG were generated from calibration products describing the resolution for that set of gratings and then the RMF was generated in the same fashion as those for the HETG. Formats for the RMF files can be found in the *Response Tool Design Spec.* `http://icxc.harvard.edu/icd/HTML/index.html` .

2.4 Data Files

The RMF files can be found on the CFA computers at

```
/data/da/caldb/tel/grating/hetg/cpf/rmf/
 HETG/ACIS-S RMFs (See $CALDB/data/chandra/tel/grating/hetg/cpf/rmf/)

 acisheg1D1999-07-22rmfN0001.fits
 acisheg2D1999-07-22rmfN0001.fits
 acisheg3D1999-07-22rmfN0001.fits
 acismeg1D1999-07-22rmfN0001.fits
 acismeg2D1999-07-22rmfN0001.fits
 acismeg3D1999-07-22rmfN0001.fits


/data/da/caldb/tel/grating/letg/cpf/rmf/:
 LETG/HRC-S RMFs (See $CALDB/data/chandra/tel/grating/letg/cpf/rmf/)

 hrcleg1D1999-07-22rmfN0001.fits
 hrcleg2D1999-07-22rmfN0001.fits
 hrcleg3D1999-07-22rmfN0001.fits
```

or at MIT

`/nfs/wiwaxia/d4/ASC/data/caldb/data/axaf/grating/hetg/cpf/grmf`

for the HETG and for the LETG with the same names as above.

`/nfs/wiwaxia/d4/ASC/data/caldb/data/axaf/grating/letg/cpf/grmf/`

The LSF libraries for the dispersion and cross dispersion direction can be found at MIT at

`/nfs/wiwaxia/d4/ASC/data/caldb/data/axaf/grating/hetg/cpf/`

and are

```
hegD1999-10-07rpsfDispN0000.fits
hegD1999-10-07rpsfX-dispN0000.fits
megD1999-10-07rpsfDispN0000.fits
megD1999-10-07rpsfX-dispN0000.fits
```

for the LETG

`/nfs/wiwaxia/d4/ASC/data/caldb/data/axaf/grating/letg/cpf/`

and are

```
legD1999-10-07rpsfDispN0000.fits
legD1999-10-07rpsfX-dispN0000.fits
```

on the HEAD LAN these files can be found in

`/data/axaf8/PSF/LSF/`

The EE files will be distributed in a future release.

2.5 File Formats

The file format for the data products are defined in the following ICD's (Interface Control Documents).

`The Gratings PSF Library` and `PSF Tool products ICD`

and is available at

`http://hea-www.harvard.edu/asclocal/sds/ICD/index.html`

3 The CXO Grating PSF's, LSF's and RMF's

This section we examine the reference data products generated from the simulations. First we show examples of the two dimensional images used to generate the library products, Then we examine the projected LSF and compare these LSF's statistically to a Gaussian. We fit the LSF's with Gaussian functions that represent the gross properties of the LSF's and show the deviations from the fits, and finally we show plots of the 90% encircled energy radius as a function of energy.

3.1 2-D Grating PSF Images

In this section we show examples of the two dimensional structure of the images which will be used to derive LSF's, cross-dispersion profiles and encircled energy functions in the later sections.

Figure 2 shows representative 2-D on-axis images from which the dispersion and cross-dispersion profiles are derived. Both of these images are sampled at 1 μm resolution which is 24 times better than the resolution of ACIS and the image size is 256 pixels on a side.

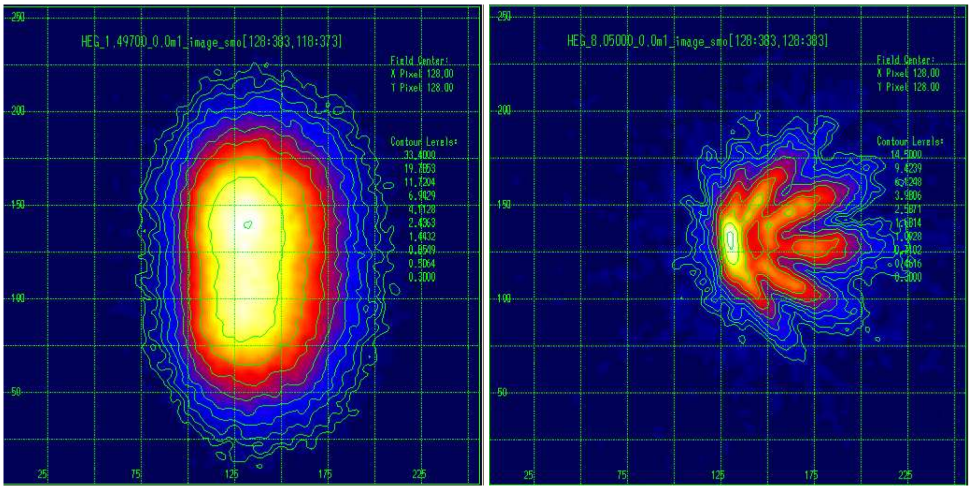

Figure 2: Two dimensional images of the HEG LSF. The left image is the 1.497 keV line and the right is the 8.05 keV. Both images are for the HEG -1 order. The pixel size is 1μm and the major tick marks are spaced at 25 μm.

3.2 Skewness and Kurtosis of the Grating LSF

Determining the line profile for a point source is fundamental for the analysis of spectrometer data and often the LSF can be described by a symmetric function. However, the line profiles from the CXO gratings are not symmetric and thus cannot, in general, be well described by a symmetric function such as a Gaussian. However, a Gaussian can describe the gross properties of the LSF, such as the width, and deviations from a Gaussian indicate how well a Gaussian can mimic the LSF. The Gaussian is symmetric about the mean, so the first deviation is asymmetry. Skewness is defined such that if more datapoints lie below the mean of the dataset it is known as negatively skewed. If the distribution is depleted of values below the mean it is positively skewed.

The second deviation from symmetry is known as kurtosis and compares the population of the tails of the dataset to that of the central region. If a distribution is more peaked than a Gaussian and/or the tails are more populated than a Gaussian then it has a positive kurtosis. If a distribution has tails less populated and/or is less peaked than a Gaussian then it has a negative kurtosis.

The skewness and kurtosis for the HEG and MEG data are shown in figure 3 for the dispersion direction. Similarly the skewness and kurtosis for the cross-dispersion direction is shown in figure 4. The skewness for the MEG and HEG data area always positive indicating that there is more power above the mean (at higher dispersion distance) when compared to a Gaussian. The HEG skewness for the dispersion direction is fairly constant rising slightly with energy from about 2.3 at 1.49 keV to $\sim$2.5 at 10 keV while that for the cross-dispersion direction range is from 1.7 up to almost 2.5. The MEG skewness ranges from 2.4 to 3.5 for the dispersion direction and from 1.2 to a value of 3.2 for the cross-dispersion direction. The kurtosis for the HEG ranges from about 4.2 at 1.49 keV to 6 at 10 keV for the dispersion direction and about 1.5 at 1.4 keV and peaks near 5 at 6.4 keV for the cross-dispersion data. The kurtosis for the MEG dispersion direction data ranges from $\sim$5 to 13 and for the cross-dispersion data ranges from zero at 1.4 keV and increases to a maximum of 10 at 6.4 keV. This indicates that the LSF has more power in the wings of the distribution than can be accounted for with a Gaussian model. The skewness and kurtosis for the plus and minus orders at 8 and 10 keV do not agree and this is caused by the low number of simulated photons at these energies. One reason that the MEG cross dispersion skewness is larger than that for the HEG is the presence of the mis-aligned MEG gratings (see `HETG Ground Calibration: version 2.0` §`6.4 Mis-Aligned Gratings`).

The skewness for the LETG LSF ranges from low of $\sim$2 up to 2.6 for the dispersion direction and from $\sim$2 to 2.7 for the cross dispersion direction. The kurtosis for the dispersion direction ranges from $\sim$2 to just below 6 and from 2 to just above 6 in the cross dispersion direction. So like the HEG and MEG LSF's the LEG LSF also deviates significantly from a Gaussian.

In summary, Gaussian fits to the grating LSF is an inadequate description for sources with significant counts in a line. The kurtosis plots above show that the LSF is too much power in the peak and/or too much power in the wings to be fit with a Gaussian. The large values of the kurtosis indicate that fitting the LSF with symmetric functions may only be a first approximation since there are large deviations from symmetry.

However, more detailed modeling with MARX (eg. by including aspect blur) may reduce these effects and will be explored more fully in a future memo. In the next section we will compare the RMF's generated with the Gaussian approximation the simulated LSF's and later to flight data.

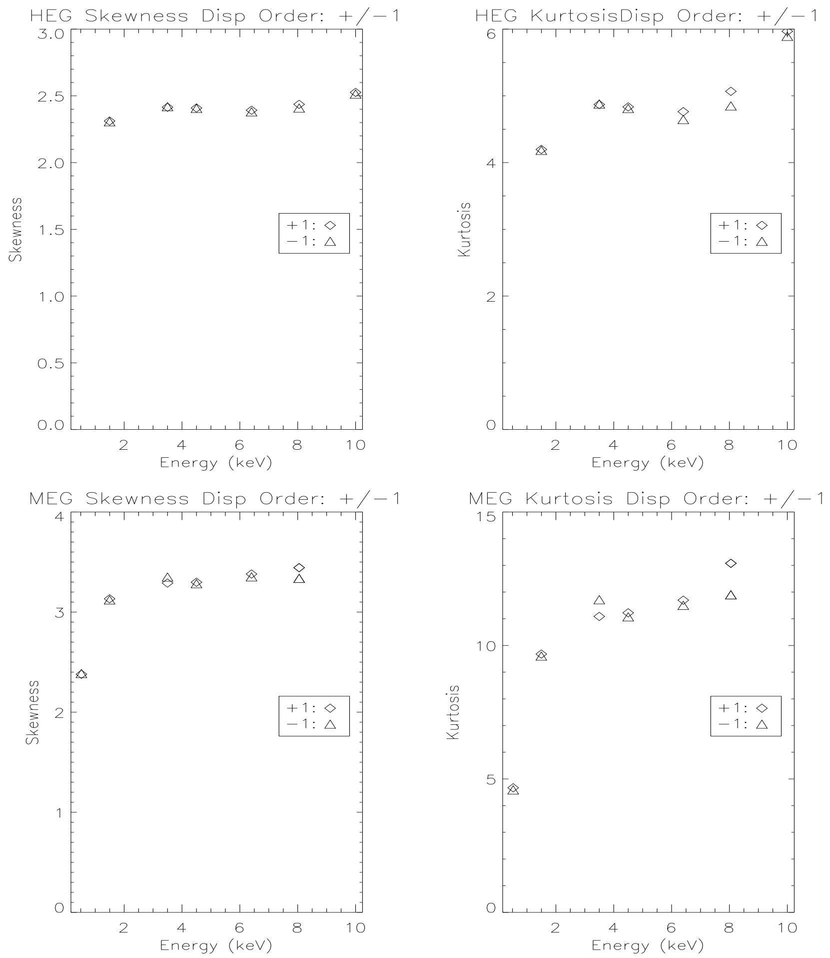

Figure 3: The skewness and kurtosis of the simulated HEG LSF (top) and MEG LSF (bottom) vs energy.

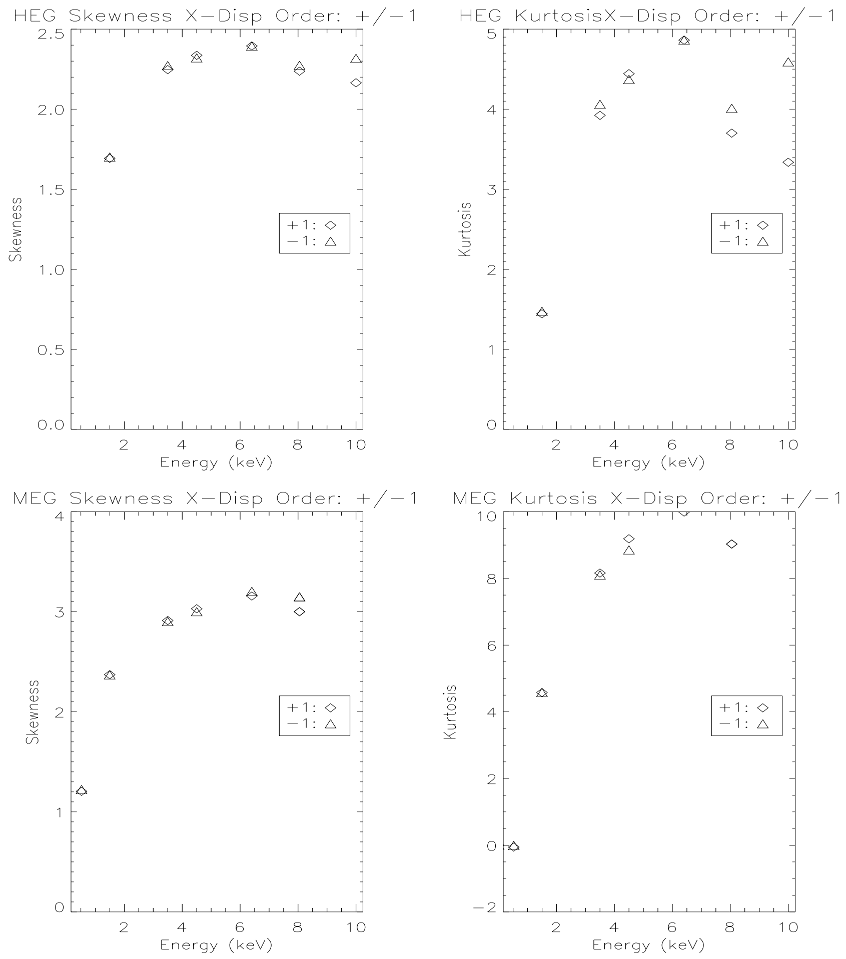

Figure 4: The skewness and kurtosis of the simulated HEG LSF (top) and MEG LSF (bottom) vs energy for the cross dispersion direction.

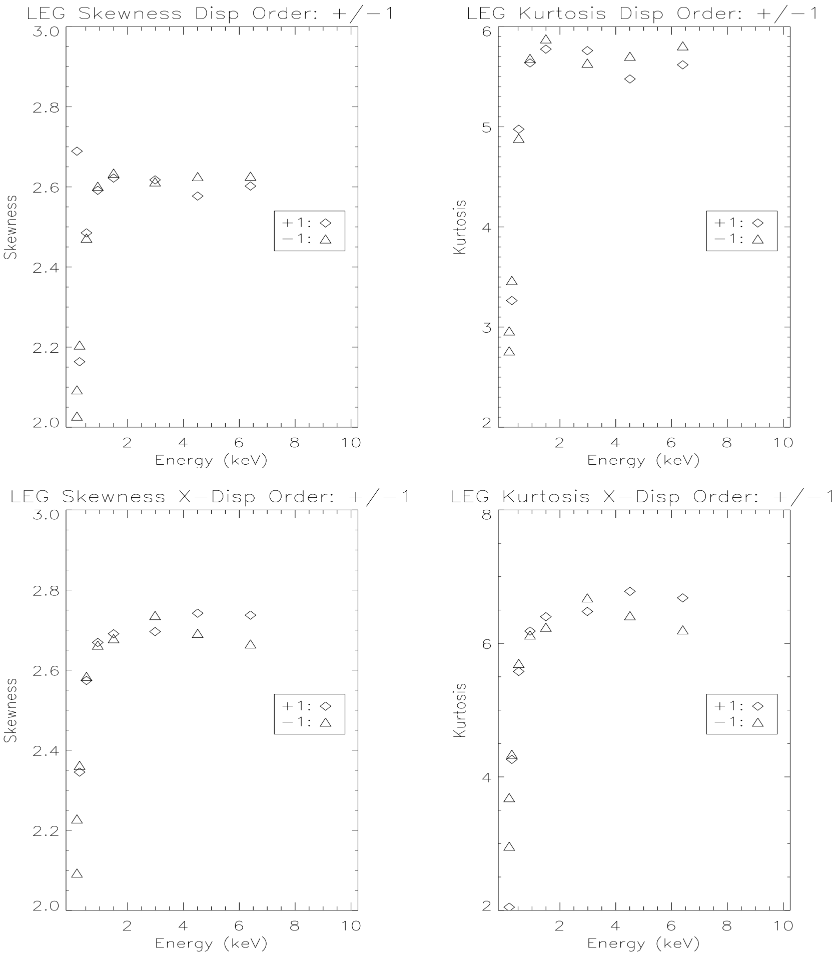

Figure 5: The skewness and kurtosis of the simulated LEG LSF vs energy for the dispersion direction (top) cross dispersion direction(bottom).

3.3 Analytic Fits to the LSF

3.3.1 Gaussian Fits

The LSF's are extracted from the simulations in the dispersion and cross-dispersion directions using the same 5.3″ region used for the library files. These profiles are then fit with a Gaussian function with the center, width, and normalization free to vary. These fits are done using the IDL fitting routine curvefit. In general the Gaussian fits the central part of the line profile reasonably well but the outer parts of the profile, the wings, are systematically broader than a Gaussian (see figures 6,7). This can be seen in the fits and the χ^2 plots where very large values of χ^2 are seen in the outer regions. The absolute value of χ^2 is determined using only statistical errors of the simulation and ignore any calibration uncertainties for this calculation.

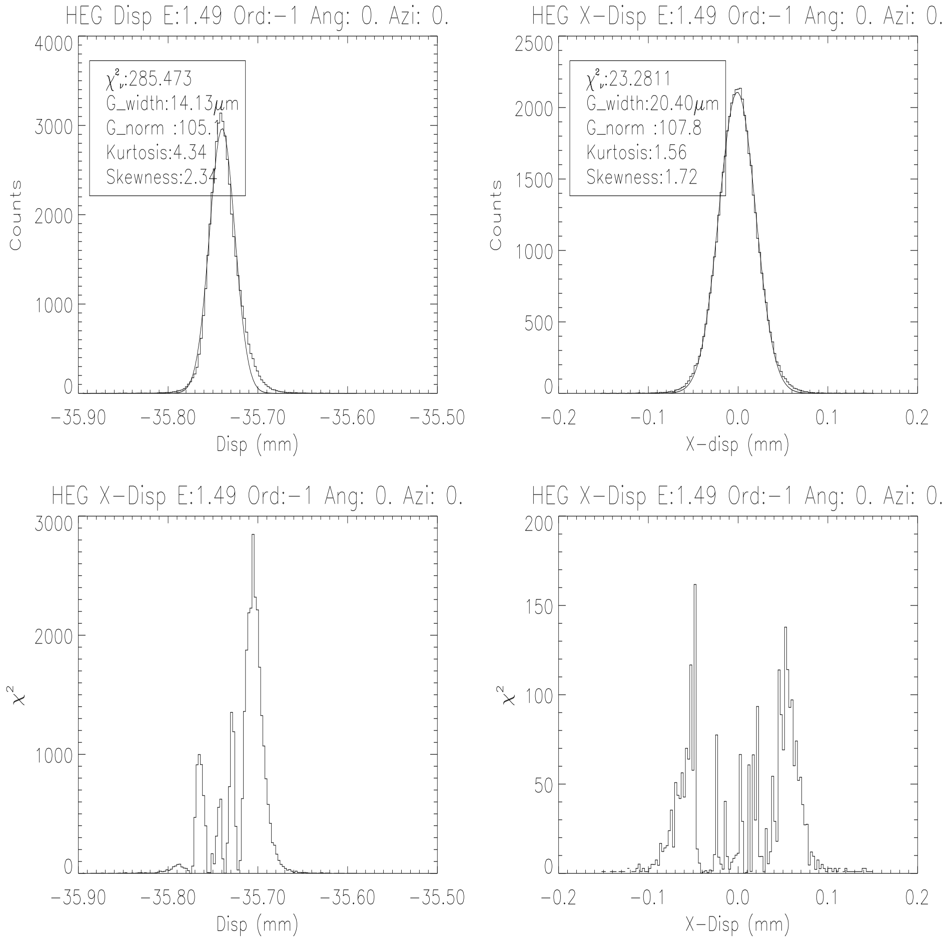

Figure 6: One dimensional on-axis dispersion and cross dispersion profiles of the HEG LSF order -1 at 1.49 keV. The left image is the dispersion profile and the right is the cross-dispersion profile. The lower plots show the χ^2 plot for the Gaussian fit to the data.

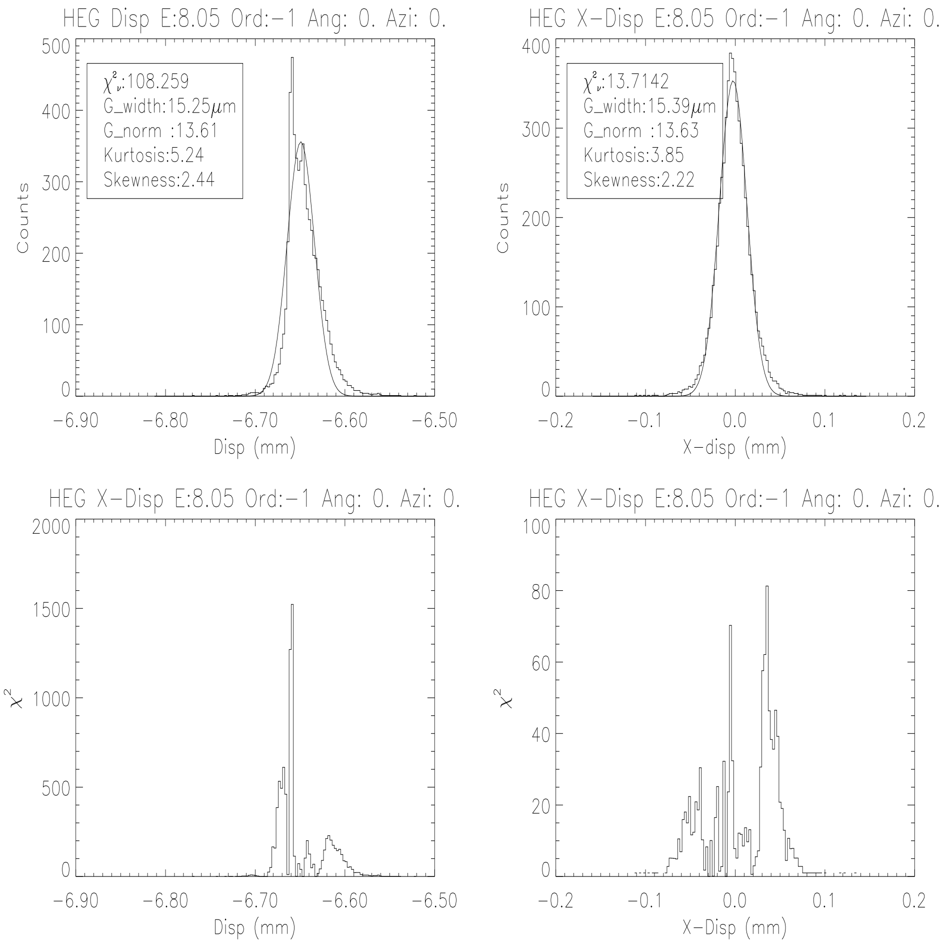

Figure 7: One dimensional on-axis dispersion and cross dispersion profiles of the HEG LSF order -1 at 8.05 keV. The left image is the dispersion profile and the right is the cross-dispersion profile. The lower plots show the χ^2 plot for the Gaussian fit to the data. The narrow, strong peak to the left of the fitted peak is from the offset mirror shell 6.

Plots of the Gaussian width vs Energy are given in Figure 8, 9, 10. The HEG and MEG data show clear trends of the Gaussian width with energy. The lowest energy (largest dispersion distance) shows the largest width which rapidly decreases to a fairly constant width for the MEG data. The HEG widths also decrease rapidly with increasing energy, show a minimum width at ~ 6.4 keV, and then shows a mild increase up to ~ 10 keV. The LETG widths (figure 10) show a steep decrease with increasing energy up to about 1 keV above which the widths are fairly constant.

Table 3.3.1 shows the resolution ($\lambda/\Delta\lambda$) (as defined in `HETG Ground Calibration: version 2.0` where $\Delta\lambda = FWHM = 2\sqrt{2ln2}\sigma$) for some of the measured lines shown in figure 8. Not surprisingly, these values agree well with pre-flight design predictions and with earlier predictions (see `http://space.mit.edu/HETG/res_power/res_power.html`).

	MEG		HEG		LEG	
Wavelength	σ	$\lambda/\Delta\lambda$	σ	$\lambda/\Delta\lambda$	σ	$\lambda/\Delta\lambda$
Å	μm		μm		μm	
67.71	···	···	···	···	11.70	1987
44.73	···	···	···	···	15.20	1010
23.42	28.8	1570	···	···	12.62	642
13.32	···	···	···	···	11.93	383
8.32	14.	767	20.5	991	11.74	242
3.54	10.9	352	14.8	443	···	···
2.75	10.5	266	14.4	340	···	···
1.94	9.65	196	14.1	234	11.74	122
1.54	10.6	146	14.9	177	···	···
1.24	···	···	15.5	136	···	···

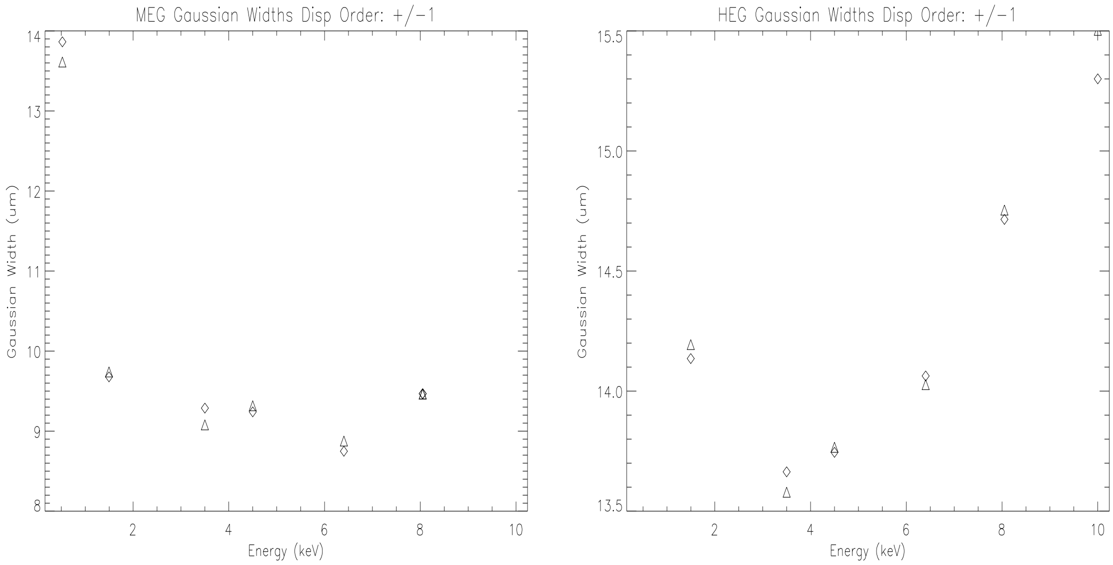

Figure 8: The dispersion width (σ) of the Gaussian fits for the HEG and MEG are plotted vs energy and the symbols are the same as in figure 3.

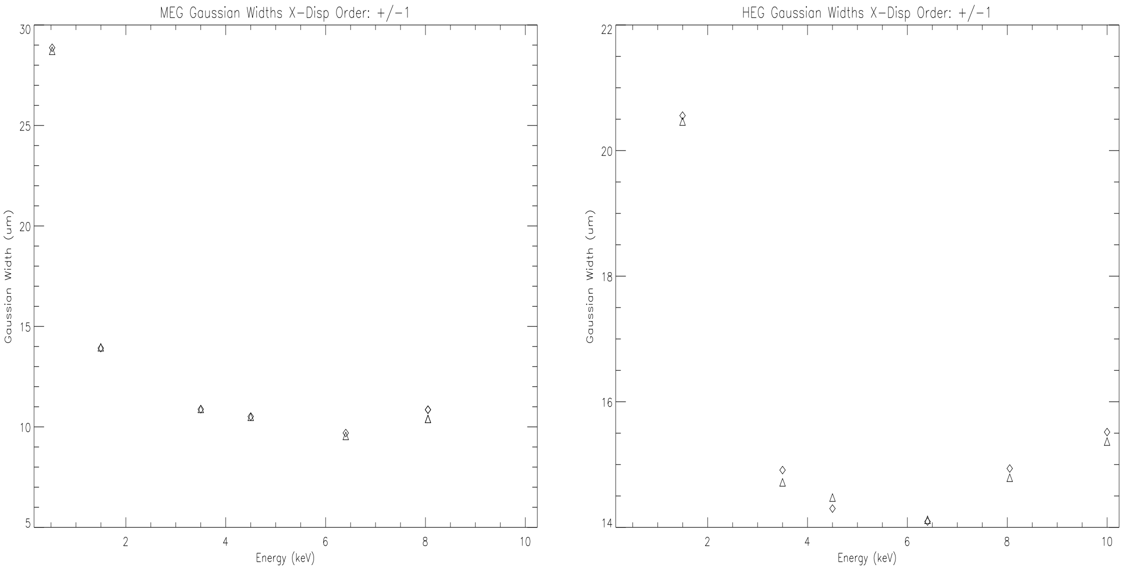

Figure 9: The cross dispersion width (σ) of the Gaussian fits for the HEG and MEG are plotted vs energy

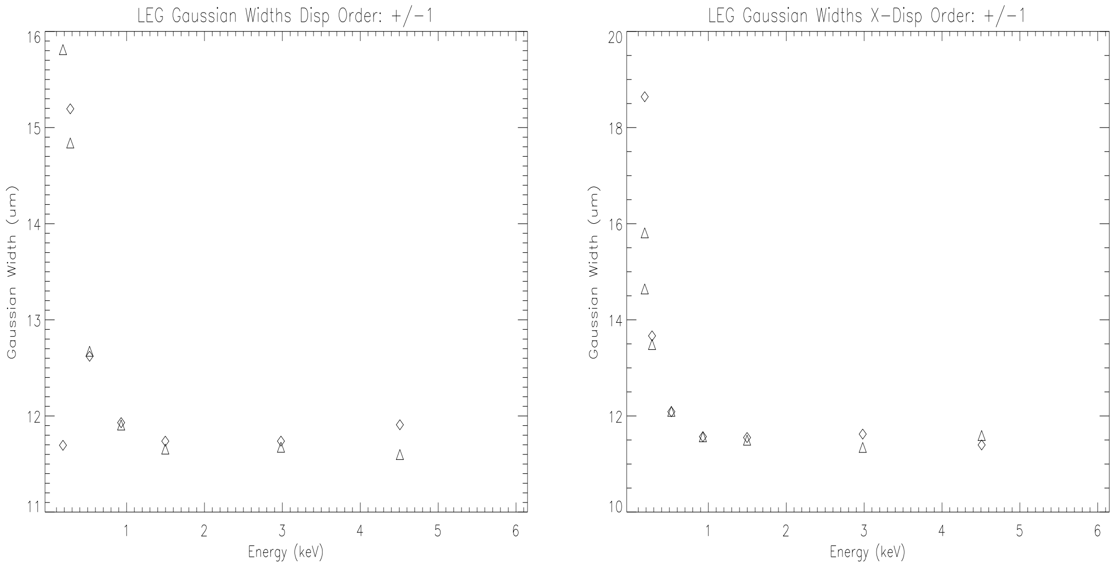

Figure 10: The width (σ) of the Gaussian fits for the LEG for the dispersion and cross dispersion are plotted vs energy

3.4 Encircled Energy

Accurate flux calibration of the extracted spectra requires knowledge of the fraction of the source photons which fall in the extraction aperture for the spectrum. This fraction, the encircled energy (EE), is modeled here with MARX data and this can be used to determine the absolute flux for a spectral line with a known extraction aperture. The width of the 90% EE radius in the cross-dispersion direction is shown below in the plots as a function of energy. For the LSF's discussed here the extraction region is always greater than the 90% EE fraction so that the correction for flux lost from the LSF is small (<0.2%). The default data extraction region for tgextract is $\sim 7''$ wide so that correction for lost photons is negligible.

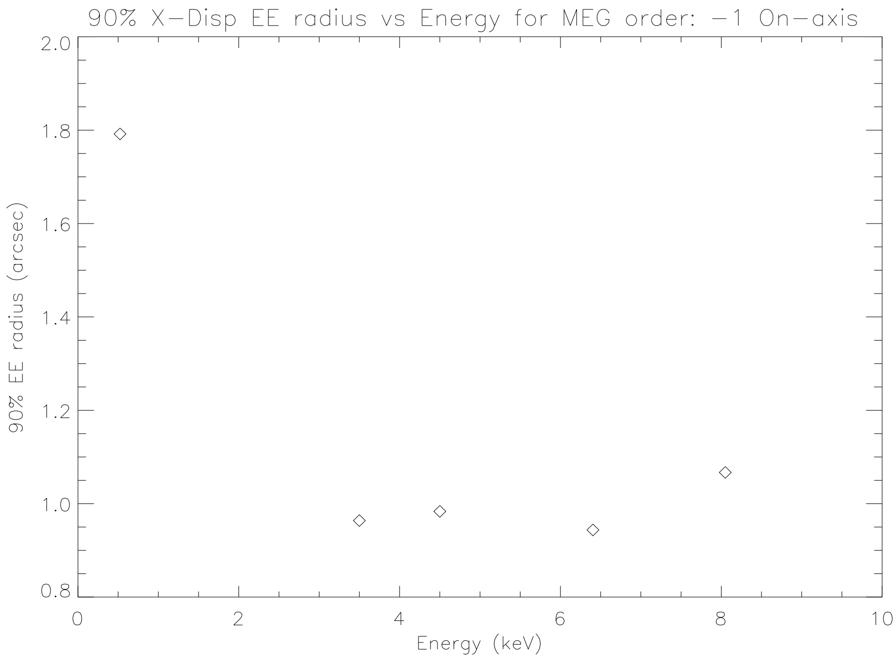

Figure 11: The 90% encircled energy radius as a function of energy for the MEG -1 order on-axis simulations.

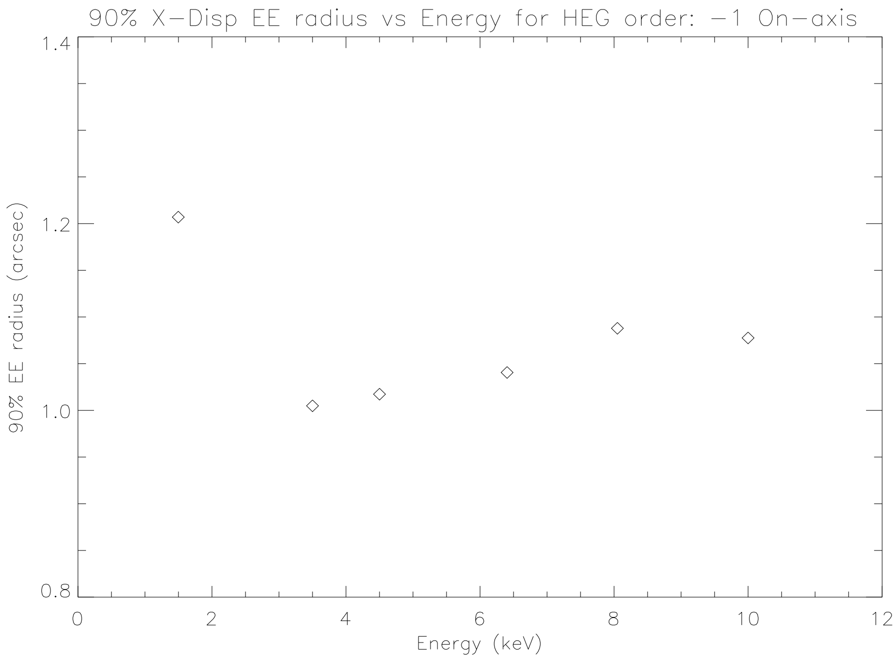

Figure 12: The 90% encircled energy radius as a function of energy for the HEG -1 order on-axis simulations.

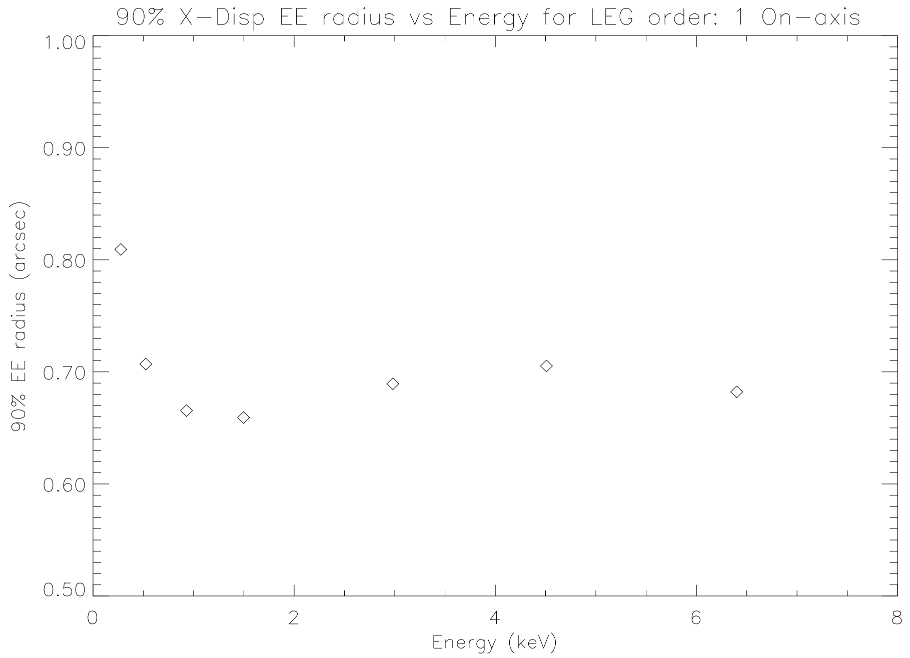

Figure 13: The 90% encircled energy radius as a function of energy for the LEG +1 order on-axis simulations.

4 On-Orbit Data and Fits

Although the detailed comparison of grating LSF models to flight data properly belongs with the calibration and IPI teams, it is instructive to compare the initial LSF library data to actual flight data. Calibration observations of the star Capella are presented below for the HETG + ACIS-S and for the LETG + HRC-S.

Observations of Capella (Obsids 1103, 1235, 1318 are merged for a total of $\sim$ 88ksec with plus and minus orders added) are fit with a Gaussian convolved with the RMF (Gaussian fits) and are shown at the top of the page in the following plots and with a δ-function convolved with the RMF (δ-function fits) and are shown in the lower part of the page. The Capella data for LETG is from obsid 1167 and has an approximate observation time of 15.2 ksec. The LETG data is fit using the RMF's described in §2.

In general, the RMF's allow accurate fitting to done with the data from the gratings. The HEG data for the Mg XII line shows no evidence of being more extended than the LSF at that energy (see figure 14 and 15). The data for the Si XIV line (figure 16 and 17) shows some evidence for a more complex structure and there may be a weak line in the wings of the Si line at higher energy. When fitting the line with a Gaussian the χ^2 was reduced by 2.5 for 16 degrees of freedom from the fit using the δ-function and is not significant (see fig 17). So both of these lines are well fit using the existing HEG RMF data.

The MEG data for Capella has significantly more counts than the HEG data and therefor should be more sensitive to an extended component in the wings. Figure 18 shows the O VIII Lyα line fit with a Gaussian and the redidual plot (lower panel) shows excess counts in the core and in the wings. This can also be seen in the 1μm fits (see figure 6). This same effect can also be seen in the fit with just the LSF (figure 19). As the spectral resolution decreases with decreasing wavelength the MEG data shows less of a need for an extended Gaussian component (Figure 20, 21, 22, and 23). The data for the Si XIV line is consistent with the LSF.

The LETG data for Capella along with the fits and residuals for Oxygen VIII Ly-α at 18.97Å and for Fe XVIII at 93.93Å are shown in figures 24, 25, 26, 26. For both of these lines the δ-function fits are broader than the fits with a Gaussian profile. The core of the line seems to be well represented by the δ-function convolved with the RMF of the instrument but the wings are not well fit with this model (see figures 25, 23).

In summary the current RMFs can be used successfully to fit flight data from the HETG aboard Chandra. Some care must be taken not to over-interpret the data low energies (high spectral resolution) given That the current RMF's have large residuals in that region. At higher energies the current RMF's provide an excellent fit to the data. For the LETG data the wings of the LSF are significant and slightly broader than the Gaussian model in the current RMF's. So any model fitting with the current RMF's for the LETG data will generate fairly substantial residuals in the wings of the lines.

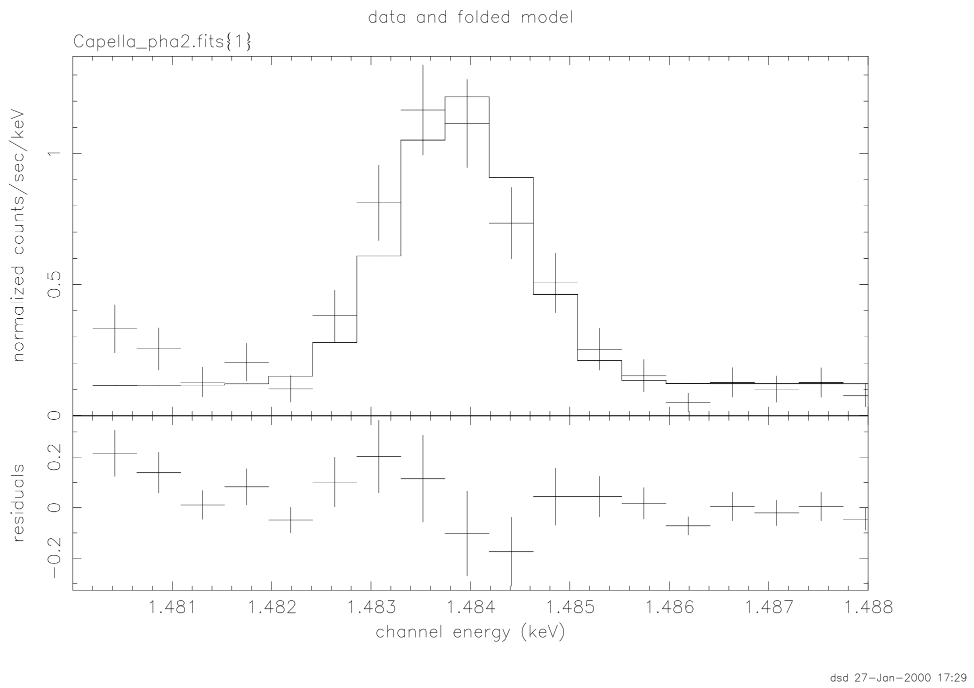

Figure 14: The Capella data for the MgXII line at 8.42Åfor HEG +1 and -1 is plotted as the crosses while the Gaussian fit is shown as the solid line. The lower panel shows the residuals of the fit.

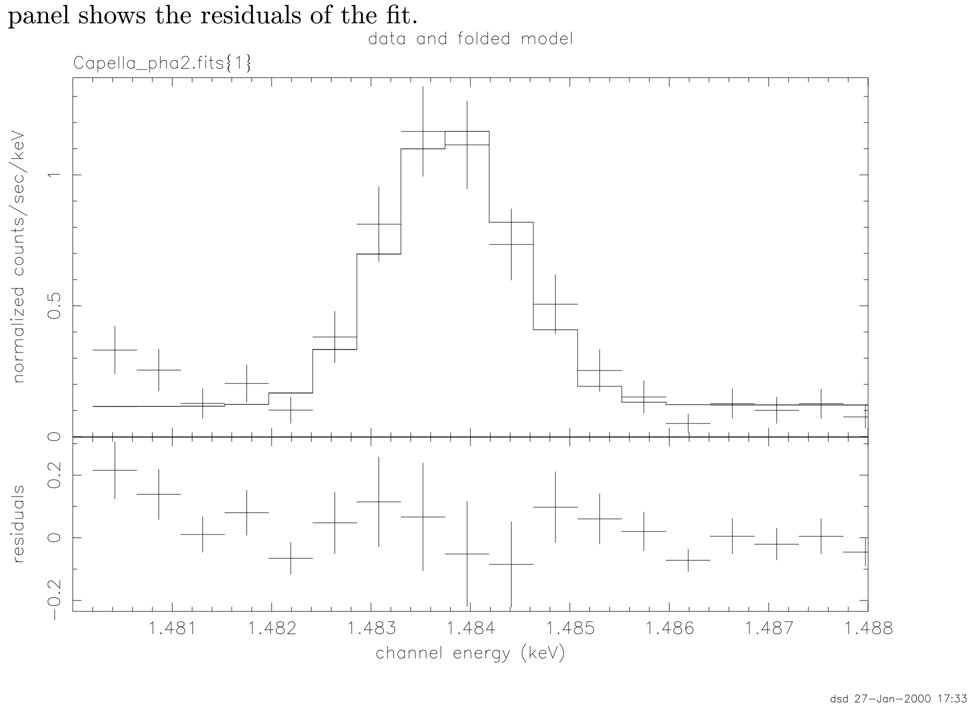

Figure 15: The Capella data for the MgXII line at 8.42Å for HEG +1 and -1 is plotted as the crosses while the solid line shows the δ-function fit. The lower panel shows the residuals of the fit.

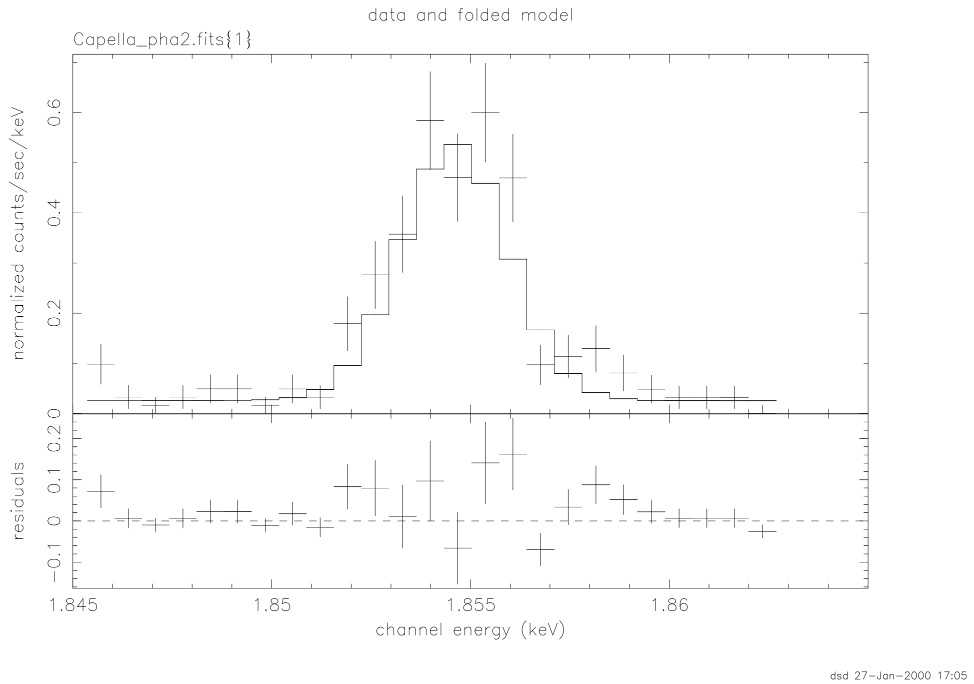

Figure 16: The Capella data for the Si line at 6.18Å , otherwise this is the same as fig 14.

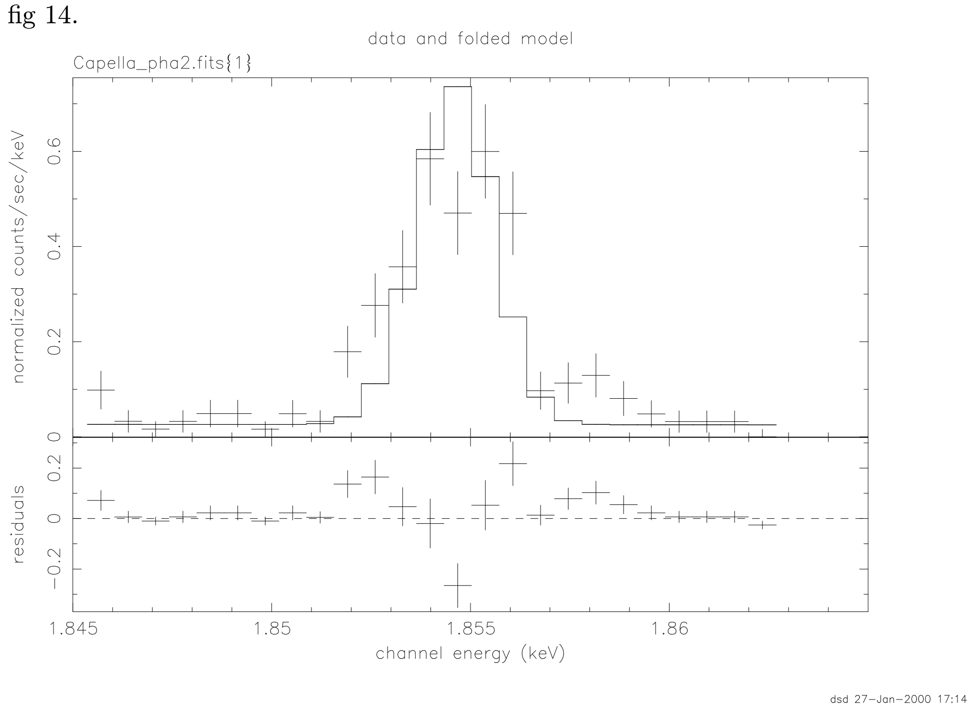

Figure 17: The Capella data for the Si line at 6.18Å with the δ-function fit plotted as the solid line, otherwise this is the same as fig 15.

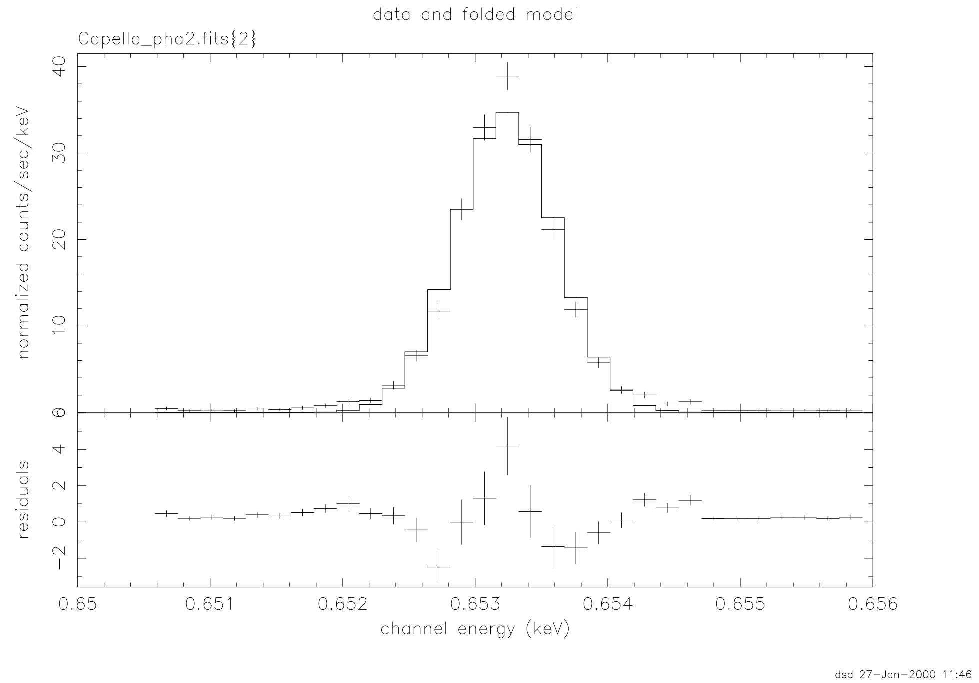

Figure 18: The Capella data for the OVIII Lyα line at 18.97Å for MEG +1 and -1 is plotted as the crosses while the Gaussian fit is shown as the solid line. The lower panel shows the residuals of the fit.

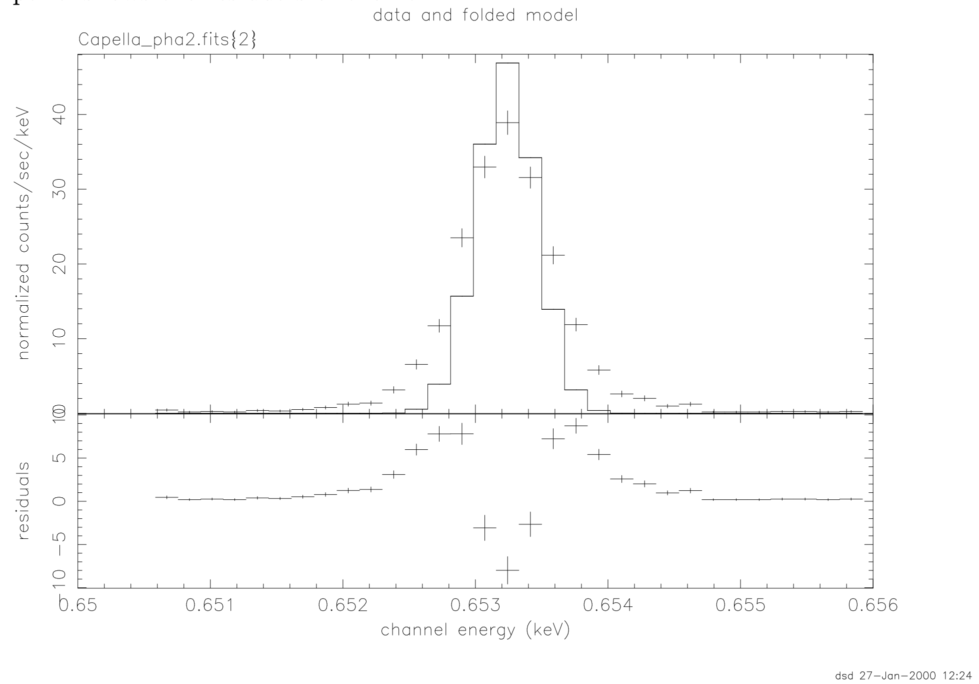

Figure 19: The Capella data for the OVIII Lyα line at 18.97Åfor MEG +1 and -1 is plotted as the crosses while the δ-function fit is shown as the solid line. The lower panel shows the residuals of the fit.

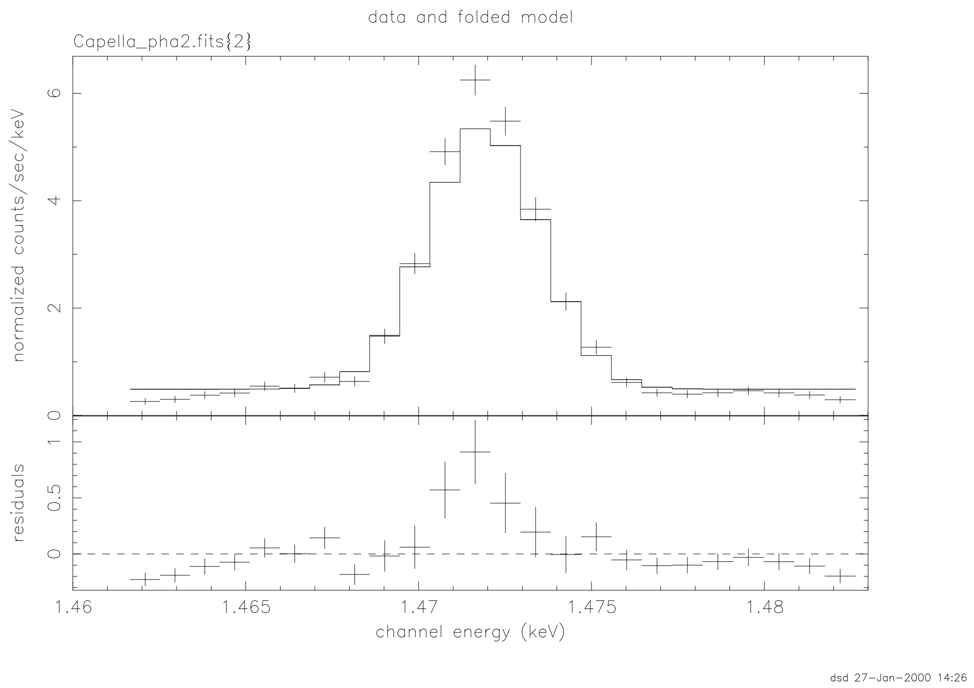

Figure 20: The Capella data for the Mg XII Lyα line at 8.42Å, otherwise this is the same as fig 18.

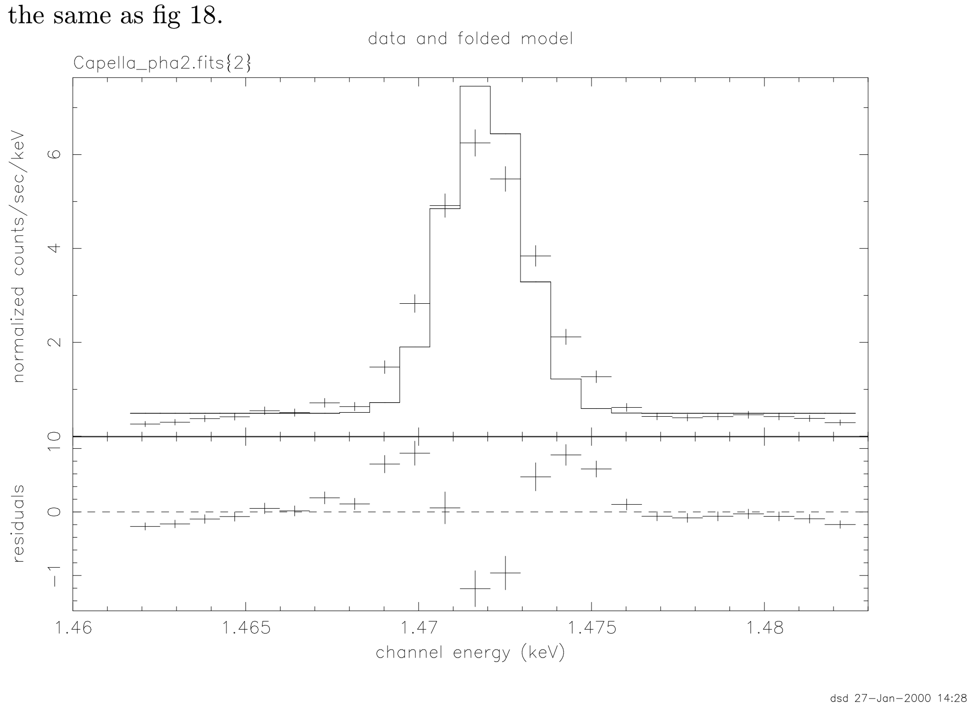

Figure 21: The Capella data for the Mg XII Lyα line at 8.42Åwith the δ-function fit shown as the solid line, otherwise this is the same as fig 18.

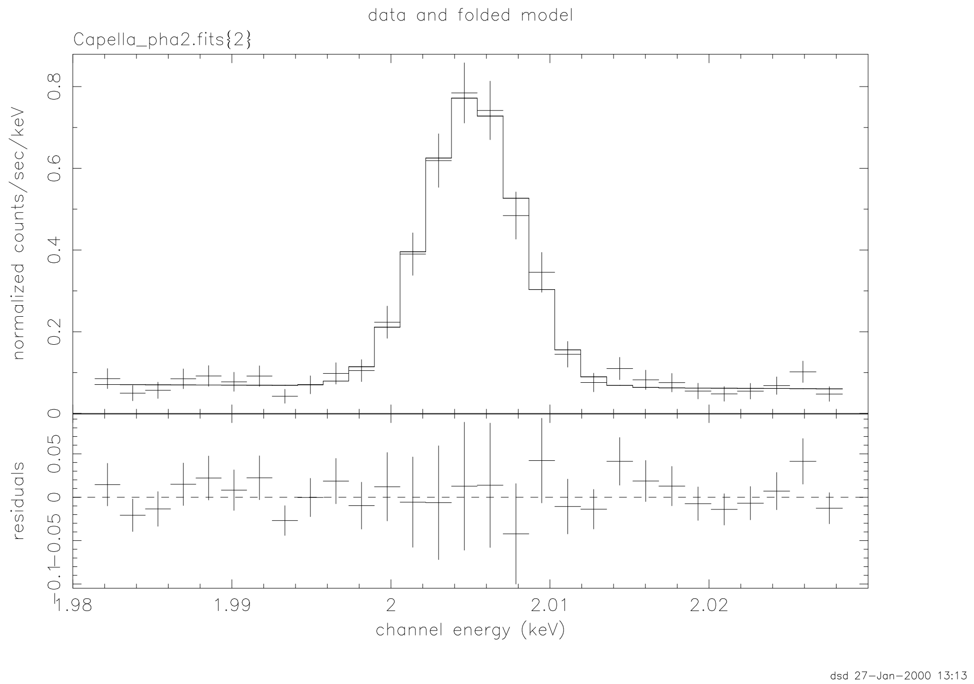

Figure 22: The Capella data for the Si XIV line at 6.18Å, otherwise this is the same as fig 18.

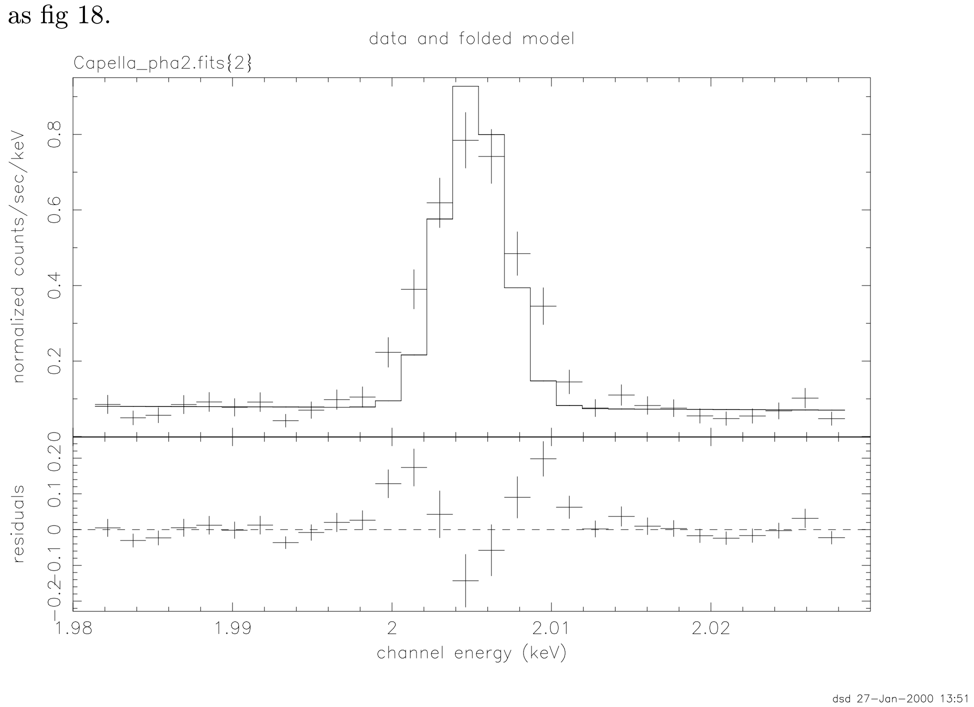

Figure 23: The Capella data for the Si XIV line at 6.18Å with the δ-function fit plotted as the solid line, otherwise this is the same as fig 18.

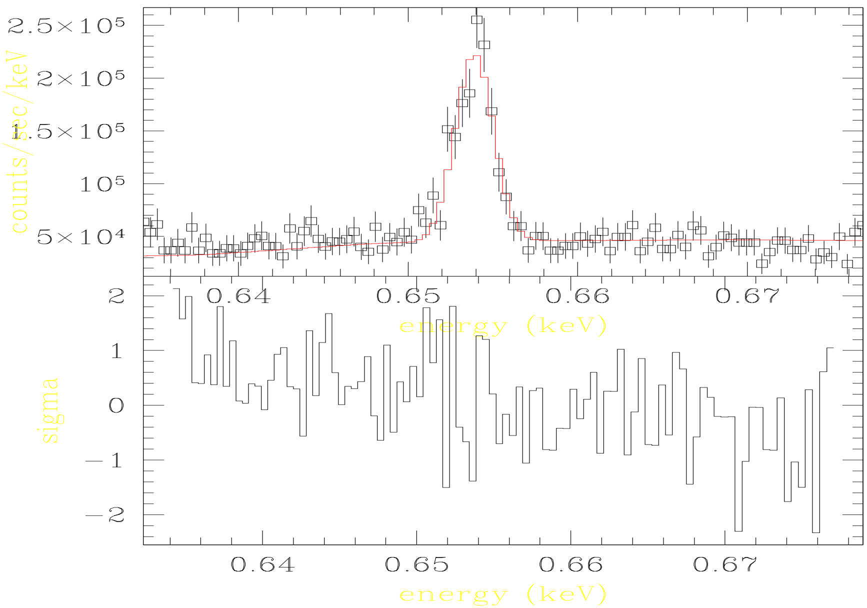

Figure 24: The LETG + HRC-S Capella data for the O VIII Lyα line at 18.97Å. The LETG data are plotted as squares and the model is the solid line.

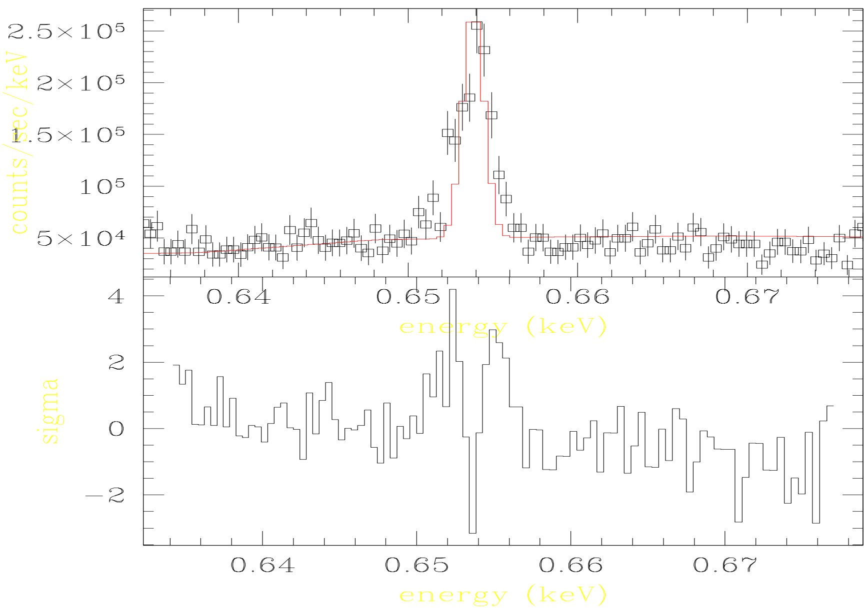

Figure 25: The Capella data for the O VIII line at 18.97Å with the δ-function fit plotted as the solid line, otherwise this is the same as fig 24.

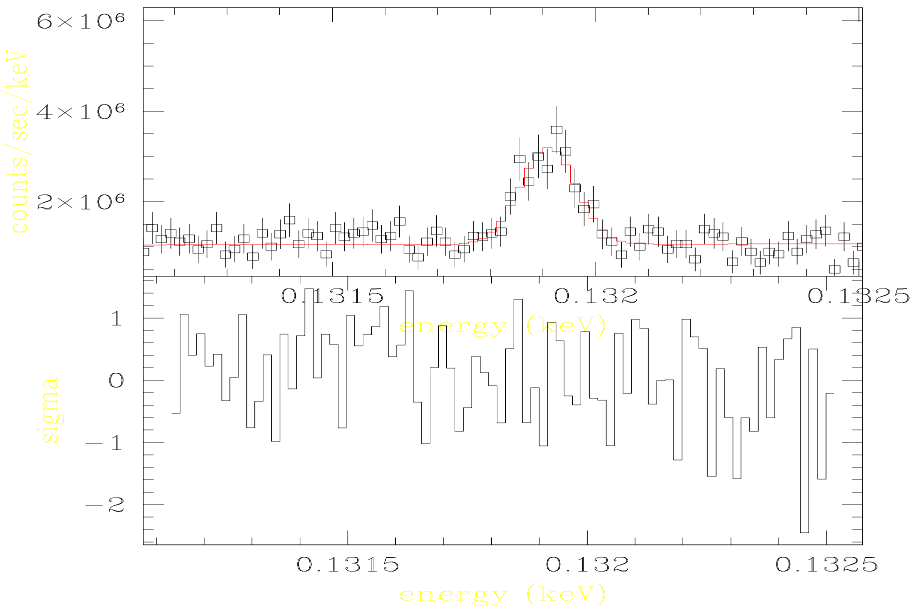

Figure 26: The LETG + HRC-S Capella data for the O VIII Lyα line at 93.93Å. The LETG data are plotted as squares and the model is the solid line.

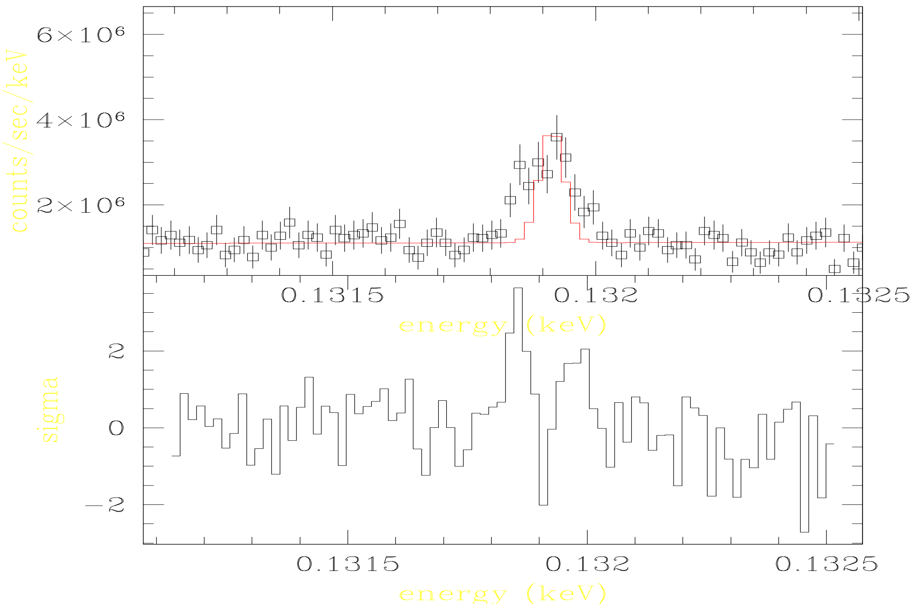

Figure 27: The Capella data for the Fe XVIII line at 93.93Å with the δ-function fit plotted as the solid line, otherwise this is the same as fig 26.

5 LSF Tools

5.1 Introduction

The following "PSF tools", in addition to their imaging functions, are also used to access the grating LSF's. Hence, in this section PSF and LSF are used interchangeably. These exist both as user callable programs and as subroutines that can be called from within other programs (eg. the ARFtool).

PSF_model requires the position of the zero order, energy, order, grating, and projection direction to determine which lsf in the library files to retrieve. If no lsf image is available at that particular position then the tool will interpolate between images in the library to obtain the best lsf to return. The order of the interpolation is to first linearly interpolate in position the four images which enclose the requested postion to obtain images at the two energies that bracket the input energy. Then these images are linearly interpolated in energy to the requested energy to obtain the final image. The final image is then resampled to the bin size requested or it can be returned with the original sampling of the library. The lsf is passed back to the calling program as a FITS image.

PSF_Frac integrates a LSF image, supplied by psf_model, within a given radius or region to obtain the fraction of the PSF within that radius. The inputs for psf_frac are the same as psf_model, since it calls psf_model to obtain the input image, with the addition of an input radius or a region mask. If a radius is given the the PSF will be integrated out to and including that radius, and if a region mask is input the the PSF fraction is the total counts within the mask divided by the total counts in the PSF/LSF image.

PSF_SIZE uses the encircled energy tables to provide an estimate of the size of the psf. The inputs are the same as those for psf_model with the addition of an EE fraction. This program uses the EE tables, instead of calling psf_model, and interpolates the EE tables in the same manner, linear interpolation in the same order as psf_model interpolates the images. This interpolated EE table is then read to determine at what radius the input EE fraction is obtained.

5.2 Documentation

There is a help file associated with each of the tools which describes the syntax for the tool, the input parameters, the output from the tool, and the algorithm. This help file is written by the developer and reviewed by the scientist resonsible for the tools and are available with the CXC data system.

5.3 Other Relevent Documents

The coordinate systems used by the grating psf tools are described in

CXC Coordinate Systems by J. McDowell
`http://hea-www.harvard.edu/asclocal/sds/docs/jsmdocs/ps/SDS02.ps`

6 Caveats

This section lists issues that are beyond the scope of the current LSF library files and tools.

Regions: The current implementation of the library assumes that that the region is wide enough (greater than $\sim 1''$) for the details in the core of the psf not to matter (cf. figure 17). For narrow extraction regions we will need multiple 1-D grating libraries or a full 2-dimensional grating PSF library.

Pileup: To compare the observed PSF with the theoretical PSF we assume that the observed data is corrected for all instrumental effects (eg. gain variations effective area, ...). It is not clear at the moment how to correct the observed data for pileup or to modify the LSF for the effects of pileup.

Frame Transfer Effects: For bright sources a significant number of photons can strike the detector during the time it takes to read the CCD creating a streak in the data. The number of counts in this streak is just the ratio of the frame transfer time to the frame time. For standard TE mode data this is about 1.2% of events in the feature. The PSF tools do not account for this.

CCD Gaps: The PSF's and derived LSF's are still generated using MARX and the MARX detectors which have the detetor gaps and edges. The library avoids these gaps to generate the PSF's but this also means that we cannot generate accurate PSF near the detector edges. This will be solved when the CXC datasystem project ray tool is available and works with the gratings.

7 Issues & Future Enhancements

The following is a list of unresolved, un-reviewed, or un-implemented items:

1. More complete fits of the Capella observation for the LETG needs to be added.
2. A more complete section describing the encircled energy and how it will affect LSF/RMF fitting and the ARF needs to be included.
3. All plots should uniformly use Å.
4. Create new LSF/RMF products with MARX 2.50 with nominal parameters
5. Tool for LSF to grating RMF needs to be developed.
6. Libraries for different cross-dispersion extraction widths needs to be generated.
7. Ablility to use windows with constant EE fraction which would require a shaped (bowtie-like) region.
8. Interpolation between the ARD with fixed regions to arbitary sized regions.
9. A DS tool to create a constant EE and constant width AARF (an ARF containing the PSF fraction in a region) will also need to be defined and developed.